

# Spectral Functions from Hadronic $\tau$ Decays and QCD

Michel Davier  
 Laboratoire de l'Accélérateur Linéaire  
 IN2P3/CNRS et Université de Paris-Sud  
 91898 Orsay, France  
 E-mail: [davier@lal.in2p3.fr](mailto:davier@lal.in2p3.fr)

Hadronic decays of the  $\tau$  lepton provide a clean environment to study hadron dynamics in an energy regime dominated by resonances. The interesting information is captured in the spectral functions. Recent results from ALEPH on exclusive channels are presented, with emphasis on the  $\pi\pi^0$  final state which plays a crucial role for the determination of the hadronic contribution to the muon anomalous magnetic moment. A comparison between  $2\pi$  spectral functions obtained in  $\tau$  decays (after corrections for isospin-breaking) and  $e^+e^-$  annihilation reveals some discrepancy in the line shape of the  $\rho$  resonance which can be attributed to different pole mass values for the charged and neutral  $\rho$ 's, which are determined through a robust fitting procedure. However, after applying this correction, the normalization of the two spectral functions differ by 3.3%. Inclusive spectral functions are the basis for QCD analyses, which deliver an accurate determination of the strong coupling constant, quantitative information on nonperturbative contributions and a measurement of the mass of the strange quark.

## 1. Introduction

Hadrons produced in  $\tau$  decays are born out of the charged weak current, *i.e.* out of the QCD vacuum, which guarantees that hadronic physics factorizes. These processes are then completely characterized for each decay channel by a spectral function which can be directly extracted from the invariant mass spectra of the final state. Furthermore, the produced hadronic systems have  $I = 1$  and spin-parity  $J^P = 0^+, 1^-$  (V) and  $J^P = 0^-, 1^+$  (A). Isospin symmetry (CVC) connects the  $\tau$  and  $e^+e^-$  annihilation spectral functions.

Hadronic  $\tau$  decays are a clean probe of hadron dynamics in an interesting energy region dominated by resonances. However, perturbative QCD can be seriously considered due to the relatively large  $\tau$  mass. Samples of  $\sim 4 \times 10^5$  measured decays are available in each LEP experiment and CLEO. Conditions for low systematic uncertainties are particularly well met at LEP: measured samples have small non- $\tau$  backgrounds ( $\sim 1\%$ ) and large selection efficiency (92%), for example in ALEPH.

## 2. Spectral Functions from ALEPH

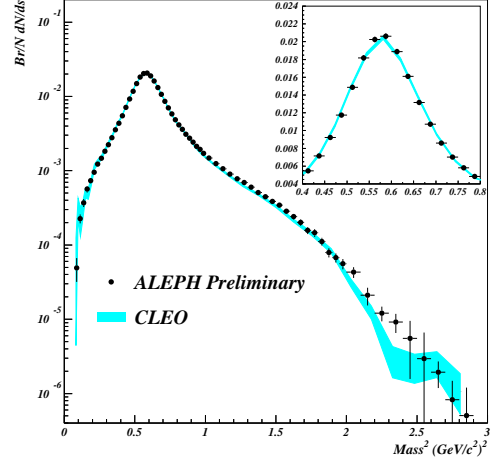
Preliminary spectral functions based on the full LEP1 statistics are available from ALEPH. The corresponding results [2] for the branching fractions which provide the absolute normalization for the spectral functions are given in Table 1. The analysis uses an improved treatment of photons as compared to the published analyses based on a reduced sample [3,4]. Spectral functions are unfolded from the measured mass spectra after background subtraction using a mass-migration matrix obtained from the simulation in order to account for detector and reconstruction biases. Backgrounds from non- $\tau\tau$  events are small ( $< 1\%$ ) and subtractions are dominated by  $\tau$  decay feedthroughs.

The spectral functions are separated into vector and axial-vector components according to the number of pions in the final state. As for final states involving  $K\bar{K}$  pairs, specific input is required to achieve the  $V - A$  separation [5].

mode	B $\pm \sigma_{\text{tot}}$ [%]	ALEPH Prel.
$e$	$17.837 \pm 0.080$	
$\mu$	$17.319 \pm 0.077$	
$\pi^-$	$10.828 \pm 0.105$	A
$\pi^- \pi^0$	$25.471 \pm 0.129$	V
$\pi^- 2\pi^0$	$9.239 \pm 0.124$	A
$\pi^- 3\pi^0$	$0.977 \pm 0.090$	V
$\pi^- 4\pi^0$	$0.112 \pm 0.051$	A
$\pi^- \pi^- \pi^+$	$9.041 \pm 0.097$	A
$\pi^- \pi^- \pi^+ \pi^0$	$4.590 \pm 0.086$	V
$\pi^- \pi^- \pi^+ 2\pi^0$	$0.392 \pm 0.046$	A
$\pi^- \pi^- \pi^+ 3\pi^0$	$0.013 \pm 0.010$	V
$3\pi^- 2\pi^+$	$0.072 \pm 0.015$	A
$3\pi^- 2\pi^+ \pi^0$	$0.014 \pm 0.009$	V
$\pi^- \pi^0 \eta$	$0.180 \pm 0.045$	V
$(3\pi)^- \eta$	$0.039 \pm 0.007$	A
$a_1^- (\rightarrow \pi^- \gamma)$	$0.040 \pm 0.020$	A
$\pi^- \omega (*)$	$0.253 \pm 0.018$	V
$\pi^- \pi^0 \omega (*)$	$0.048 \pm 0.009$	A
$(3\pi)^- \omega (*)$	$0.003 \pm 0.003$	V
$K^- K^0$	$0.163 \pm 0.027$	V
$K^- \pi^0 K^0$	$0.145 \pm 0.027$	$(94^{+6}_{-8})\% A$
$\pi^- K^0 \bar{K}^0$	$0.153 \pm 0.035$	$(94^{+6}_{-8})\% A$
$K^- K^+ \pi^-$	$0.163 \pm 0.027$	$(94^{+6}_{-8})\% A$
$(K \bar{K} \pi \pi)^-$	$0.050 \pm 0.020$	$(50 \pm 50)\% A$
$K^-$	$0.696 \pm 0.029$	S
$K^- \pi^0$	$0.444 \pm 0.035$	S
$\bar{K}^0 \pi^-$	$0.917 \pm 0.052$	S
$K^- 2\pi^0$	$0.056 \pm 0.025$	S
$K^- \pi^+ \pi^-$	$0.214 \pm 0.047$	S
$\bar{K}^0 \pi^- \pi^0$	$0.327 \pm 0.051$	S
$(K 3\pi)^-$	$0.076 \pm 0.044$	S
$K^- \eta$	$0.029 \pm 0.014$	S

Table 1

Branching fractions in  $\tau$  decays from the ALEPH experiment [2,5]. Apart from the two leptonic channels, the other modes are labeled according to their nonstrange vector (V), nonstrange axial-vector (A), and strange (S) hadronic final states. The  $\omega$  decay modes marked (\*) are electromagnetic ( $\pi^0 \gamma$ ,  $\pi^+ \pi^-$ ). The branching fractions for  $\pi^- \pi^- \pi^+ 3\pi^0$  and  $a_1^- (\rightarrow \pi^- \gamma)$  are estimates, while those for  $(3\pi)^- \eta$  and  $(3\pi)^- \omega$  are from CLEO [6].

Figure 1. The comparison between ALEPH and CLEO spectral functions in the  $\pi\pi^0$  mode.

### 3. The $2\pi$ Vector State

#### 3.1. The Data

The spectral function from  $\tau \rightarrow \nu_\tau \pi^- \pi^0$  from the full-LEP1 ALEPH analysis ( $\sim 10^5$  events) is available. It is in good agreement with the results from CLEO [7] as shown in Fig. 1. The statistics is comparable in the two cases, however due to a flat acceptance in ALEPH and a strongly increasing one in CLEO, ALEPH data are more precise below the  $\rho$  peak, while CLEO is more precise above. Note that, due to the unfolding procedure, neighbouring data points are strongly correlated.

#### 3.2. $\pi\pi$ Spectral Functions and $\pi$ Form Factors

It is useful to carefully write down all the factors involved in the comparison of  $e^+e^-$  and  $\tau$  spectral functions in order to make explicit the possible sources of CVC breaking. On the  $e^+e^-$  side we have

$$\sigma(e^+e^- \rightarrow \pi^+\pi^-) = \frac{4\pi\alpha^2}{s} v_0(s) \quad (1)$$

$$v_0(s) = \frac{\beta_0^3(s)}{12\pi} |F_\pi^0(s)|^2$$

where  $\beta_0^3(s)$  is the threshold kinematic factor and  $F_\pi^0(s)$  the pion form factor. On the  $\tau$  side, the physics is contained in the hadronic mass distribution through

$$\begin{aligned} \frac{1}{\Gamma} \frac{d\Gamma}{ds}(\tau \longrightarrow \pi^- \pi^0 \nu_\tau) &= \\ \frac{6\pi |V_{ud}|^2 S_{EW}}{m_\tau^2} \frac{B_e}{B_{\pi\pi^0}} C(s) v_-(s) &\quad (2) \\ v_-(s) &= \frac{\beta_-^3(s)}{12\pi} |F_\pi^-(s)|^2 \\ C(s) &= \left(1 - \frac{s}{m_\tau^2}\right) \left(1 + \frac{2s}{m_\tau^2}\right) \end{aligned}$$

where  $V_{ud} = 0.9748 \pm 0.0010$  denotes the CKM weak mixing matrix element [1] and  $S_{EW}$  accounts for electroweak radiative corrections (see below). SU(2) symmetry implies  $v_-(s) = v_0(s)$ .

Experiments on  $\tau$  decays measure the rate inclusive of radiative photons, *i.e.* for  $\tau \rightarrow \nu_\tau \pi \pi^0(\gamma)$ . The measured spectral function is thus  $v_-^*(s) = v_-(s) G(s)$ , where  $G(s)$  is a radiative correction, computed using scalar QED.

Several levels of SU(2) breaking can be identified:

- *electroweak radiative corrections to  $\tau$  decays* are contained in the  $S_{EW}$  factor [8,9] which is dominated by short-distance effects. As such it is expected to be weakly dependent on the specific hadronic final state, as verified in the  $\tau \rightarrow (\pi, K) \nu_\tau$  channels [10]. Recently, detailed calculations have been performed for the  $\pi\pi^0$  channel [11] which also confirm the relative smallness of the long-distance contributions. The total correction is

$$S_{EW} = \frac{S_{EW}^{\text{had}} S_{EM}^{\text{had}}}{S_{EM}^{\text{lep}}} \quad (3)$$

where  $S_{EW}^{\text{had}}$  is the leading-log short-distance electroweak factor (which vanishes for leptons) and  $S_{EM}^{\text{had,lep}}$  are the nonleading electromagnetic corrections. The latter corrections are calculated in Ref. [9] at the quark

level and in Ref. [11] at the hadron level for the  $\pi\pi^0$  decay mode, and in Ref. [8,9] for leptons. The total correction amounts [14] to  $S_{EW}^{\text{inclu}} = 1.0198 \pm 0.0006$  for the inclusive hadron decay rate and  $S_{EW}^{\pi\pi^0} = (1.0232 \pm 0.0006) S_{EM}^{\pi\pi^0}(s)$  for the  $\pi\pi^0$  decay mode, where  $S_{EM}^{\pi\pi^0}(s)$  is an  $s$ -dependent radiative correction [11].

- *the pion mass splitting* breaks isospin symmetry in the spectral functions [12,13] since  $\beta_-(s) \neq \beta_0(s)$ .
- symmetry is also broken in *the pion form factor* [12,11] from the  $\pi$  mass splitting.
- a similar effect is expected from *the  $\rho$  mass splitting*. The theoretical expectation [16] gives a limit ( $< 0.7$  MeV), but it is really only a rough estimate. Thus the question must be investigated experimentally, the best approach being the explicit comparison of  $\tau$  and  $e^+e^- 2\pi$  spectral functions, after correction for the other isospin-breaking effects.
- explicit *electromagnetic decays* such as  $\pi\gamma$ ,  $\eta\gamma$ ,  $l^+l^-$  and  $\pi\pi\gamma$  introduce some small difference between the widths of the charged and neutral  $\rho$ 's.
- isospin violation in the strong amplitude through the *mass difference between  $u$  and  $d$  quarks* is expected to be negligible.

### 3.3. Fitting the $2\pi$ Spectral Functions: the $\rho$ mass splitting

The  $2\pi$  spectral function is dominated by the wide  $\rho$  resonance, parametrized following Gounaris-Sakurai [15] (GS) which takes into account analyticity and unitarity properties.

The pion form factor is fit with interfering amplitudes from  $\rho(770)$ ,  $\rho'(1450)$  and  $\rho''(1700)$  vector mesons with relative strengths 1,  $\beta$  and  $\gamma$  (real numbers). A phase  $\phi_\beta$  is also considered, since the relative phase of the  $\rho$  and  $\rho'$  amplitude is a priori unknown. The much smaller relative amplitude for the  $\rho''$  is assumed to be real. In practice we fit  $F_\pi^0(s)$  from  $e^+e^-$  data and  $F_\pi^-(s)$  from the  $\tau$

spectral function duly corrected for SU(2) breaking, however only for the spectral function  $\beta^3$  factor, for the  $S_{EW}$  factor, and for the long-distance radiative correction  $G_{EM}(s)$ . In this way, the mass and width of the dominating  $\rho$  resonance in the two isospin states can be unambiguously determined. All  $e^+e^-$  data are used, including the recently corrected precise results from CMD-2 [17,18]. On the  $\tau$  side, the accurate data from ALEPH and CLEO are used.

The systematic uncertainties are included in the fits through appropriate covariance matrices. The  $\rho$  mass systematic uncertainty in  $\tau$  data is mostly from calibration (0.7 MeV for ALEPH and 0.9 MeV for CLEO). The corresponding uncertainties on the  $\rho$  width are 0.8 and 0.7 MeV. Both mass and width determinations are limited by systematic uncertainties in  $\tau$  data, however they can be safely assumed to be uncorrelated between ALEPH and CLEO.

Due to the large event statistics, the fits are quite sensitive to the precise line shape and to the interference between the different amplitudes. Of course,  $\rho - \omega$  interference is included for  $e^+e^-$  data only and the corresponding amplitude ( $\alpha_{\rho\omega}$ ) is fit, together with its relative phase. The upper range of the fit is taken at 2.4 GeV<sup>2</sup> in the  $\tau$  data in order to avoid the kinematic end-point of the  $\tau$  spectral function where large corrections are applied. The  $e^+e^-$  data are fit up to 3.6 GeV<sup>2</sup>, so that the information on the  $\rho''$  comes essentially from  $e^+e^-$  data.

It is customary in the Novosibirsk analyses to define  $F_\pi$  including the vacuum polarization (both leptonic and hadronic) in the photon propagator. Such a prescription is not desirable when studying the real hadronic structure of the pion, and incorrect when comparing to the  $\tau$  case where these contributions are absent. Removing vacuum polarization in the fit to CMD-2  $|F_\pi|^2$  data (Table 2) yields a  $\rho^0$  mass 1.1 MeV lower. Subsequent fits are done excluding vacuum polarization.

It turns out that the resulting  $\rho$  masses and widths are quite sensitive to the strength of the  $\rho'$  and  $\rho''$  amplitudes,  $\beta$  and  $\gamma$ . So, depending on the type of fit, the derived values can exhibit some systematic shifts. The  $e^+e^-$  and  $\tau$

	VP removed	VP included
$m_\rho$	$774.4 \pm 0.6$	$775.5 \pm 0.6$
$\Gamma_\rho$	$146.7 \pm 1.3$	$145.4 \pm 1.3$
$\alpha_{\rho\omega}$	$(1.83 \pm 0.14) 10^{-3}$	$(1.51 \pm 0.14) 10^{-3}$
$\beta$	$0.079 \pm 0.006$	$0.084 \pm 0.006$
$\phi_\beta$	[180]	[180]
$m_{\rho'}$	[1465]	[1465]
$\Gamma_{\rho'}$	[310]	[310]
$\gamma$	[0]	[0]
$\chi^2/\text{DF}$	38/39	34/39

Table 2

Fits to CMD-2  $|F_\pi|^2$  data [17] using the Gounaris-Sakurai parametrization of the  $\rho$ ,  $\rho'$  resonances for two definitions of the pion form factor: excluding or including the vacuum polarization in the photon propagator. A mass shift of 1.1 MeV is observed for the  $\rho$  mass between the two cases. The values between squared brackets are fixed in the fits. The masses and widths are in MeV and  $\phi_\beta$  in degrees.

fits yield significantly different  $\rho'$  amplitudes and phases: this is particularly true when a restricted energy range is used for the fit, as it is the case when only CMD-2 data are considered (only up to 960 MeV). In order to avoid this problem, a fit to both data sets is performed, keeping common values for the  $\rho'$  and  $\rho''$  parameters. In doing so, one neglects possible isospin-breaking effects for these states, which appears to be a reasonable assumption, as the  $\rho'$  and  $\rho''$  components can be considered as second-order with respect to the dominant investigated  $\rho$  amplitude.

The differences between the masses and widths of the charged and neutral  $\rho$ 's in the common fit are found to be

$$m_{\rho^-} - m_{\rho^0} = (2.3 \pm 0.8) \text{ MeV} \quad (4)$$

$$\Gamma_{\rho^-} - \Gamma_{\rho^0} = (0.1 \pm 1.4) \text{ MeV} \quad (5)$$

The mass splitting is somewhat larger than the theoretical prediction ( $< 0.7$  MeV) [16], but only at the  $2\sigma$  level. The expected width splitting, not taking into account any  $\rho$  mass splitting, is  $(0.7 \pm 0.3) \text{ MeV}$  [11,14]. However, if the mass

difference is taken as an experimental fact, then a larger width difference would be expected. From the chiral model of the  $\rho$  resonance [19,11], one expects

$$\Gamma_{\rho^0} = \Gamma_{\rho^-} \left( \frac{m_{\rho^0}}{m_{\rho^-}} \right)^3 \left( \frac{\beta_0}{\beta_-} \right)^3 + \Delta\Gamma_{EM} \quad (6)$$

where  $\Delta\Gamma_{EM}$  is the width difference from electromagnetic decays (as discussed above), leading to a total width difference  $(2.1 \pm 0.5)$  MeV, marginally consistent with the observed value.

Table 3 presents the results of the common fits, the quality of which can be inspected in Figs. 2 and 3.

Mass splitting for the  $\rho$  was in fact considered in our first paper where we proposed using precise  $\tau$  data to compute hadronic vacuum polarization integrals [12]. Using pre-CMD-2  $e^+e^-$  data and ALEPH  $\tau$ , a combined fit was attempted which produced a mass splitting consistent with 0 within an uncertainty of 1.1 MeV. However, the form factor from  $e^+e^-$  data still contained the vacuum polarization contribution (1.1 MeV shift, as we have seen) and we also discovered a normalization problem in our treatment of the  $\tau$  data in the combined fit. With the advent of precise CMD-2 data [17], it became apparent that differences were showing up between  $\tau$  and  $e^+e^-$  form factors. A large part of the discrepancy was removed when CMD-2 re-analyzed their data [17]. Since the  $\tau$  results from ALEPH, CLEO and OPAL have been shown to be consistent within their quoted accuracy [14,18] and since preliminary results from the radiative return analysis of KLOE [20] are in excellent agreement with the corrected CMD-2 results, the question of the  $\rho$  mass splitting can be now more reliably investigated. Table 3 presents the results of the common fit, leaving  $m_{\rho^-}$  and  $m_{\rho^0}$  as free parameters, but fixing the relationship between  $\Gamma_{\rho^-}$  and  $\Gamma_{\rho^0}$  following Eq. (6). The results, which can be visualized in Figs. 2 and 3, do not provide a good description of the data with a probability of only 0.6% to get a worse fit.

Could a  $\rho$  mass splitting account for the discrepancy [14,18] between  $e^+e^-$  and isospin-corrected  $\tau$  spectral functions? Unfortunately not! Correcting the  $\tau$  data for the mass shift us-

	$\tau$ and $e^+e^-$
$m_{\rho^-}$	$775.4 \pm 0.6$
$m_{\rho^0}$	$773.1 \pm 0.5$
$\Gamma_{\rho^-}$	$148.8 \pm 0.8$
$\Gamma_{\rho^0}$	$(146.7)$
$\alpha_{\rho\omega}$	$(2.02 \pm 0.10) 10^{-3}$
$\phi_\alpha$	$(15.3 \pm 2.0)$
$\beta$	$0.167 \pm 0.006$
$\phi_\beta$	$177.5 \pm 6.0$
$m_{\rho'}$	$1410 \pm 16$
$\Gamma_{\rho'}$	$505 \pm 53$
$\gamma$	$0.071 \pm 0.007$
$\phi_\gamma$	0.
$m_{\rho''}$	$1748 \pm 21$
$\Gamma_{\rho''}$	235
$\chi^2/\text{DF}$	394./327

Table 3

Combined fit to the pion form factor squared to  $\tau$  and  $e^+e^-$  data, vacuum polarization excluded for the latter. The parametrization of the  $\rho$ ,  $\rho'$ ,  $\rho''$  line shapes follows the Gounaris-Sakurai form. For the  $\rho$ , only  $m_{\rho^-}$ ,  $m_{\rho^0}$ , and  $\Gamma_{\rho^-}$  are fitted, while  $\Gamma_{\rho^0}$  is computed from Eq. (6). All mass and width values are in MeV and the phases are in degrees. The parameters related to  $\rho'$  and  $\rho''$  amplitudes are fitted, assuming they are identical in both data sets.

ing the Gounaris-Sakurai parametrization with  $\rho$ ,  $\rho'$  and  $\rho''$  amplitudes (but the results only depend on a Breit-Wigner-like behaviour for the  $\rho$ ) improves the consistency of the  $e^+e^-$  and  $\tau$  line shapes, but at the expense of an increased overall normalization difference: the corrected  $\tau$  data lie on average 3.3% above  $e^+e^-$  hence the bad fit. The tau estimate of  $a_\mu^{\text{had,LO}}$  increases by  $5.4 \cdot 10^{-10}$  [21], in larger disagreement with the  $e^+e^-$  estimate [18].

#### 4. Inclusive Nonstrange Spectral Functions

The  $\tau$  nonstrange spectral functions have been measured by ALEPH [3,4] and OPAL [22]. The procedure requires a careful separation of vector (V) and axial-vector (A) states involving the reconstruction of multi- $\pi^0$  decays and the proper

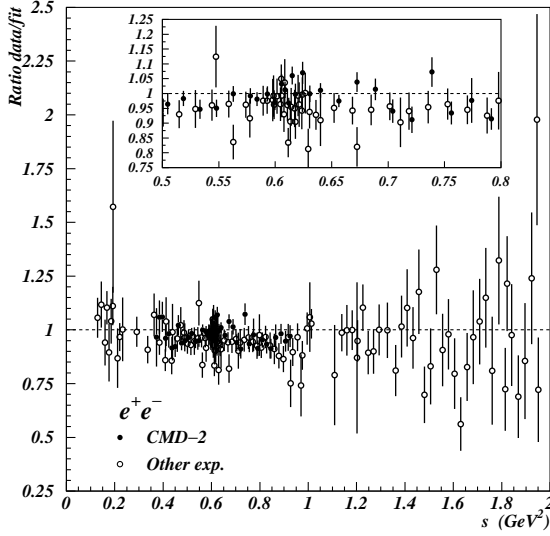


Figure 2. The ratio of the  $e^+e^-$  pion form factor squared to  $|F_\pi^0(s)|^2$  from the combined fit in Table 3.

treatment of final states with a  $K\bar{K}$  pair. The inclusive ALEPH  $V$  and  $A$  spectral functions are given in Figs. 4 and 5 with a breakdown of the respective contributions. The  $V + A$  spectral function, shown in Fig. 6 has a clear pattern converging toward a value above the parton level as expected in QCD. In fact, it displays a textbook example of global duality, since the resonance-dominated low-mass region shows an oscillatory behaviour around the asymptotic QCD expectation, assumed to be valid in a local sense only for large masses. This feature will be quantitatively discussed in the next section.

## 5. QCD Analysis of Nonstrange $\tau$ Decays

### 5.1. Motivation

The total hadronic  $\tau$  width, properly normalized to the known leptonic width,

$$R_\tau = \frac{\Gamma(\tau^- \rightarrow \text{hadrons}^- \nu_\tau)}{\Gamma(\tau^- \rightarrow e^- \bar{\nu}_e \nu_\tau)} \quad (7)$$

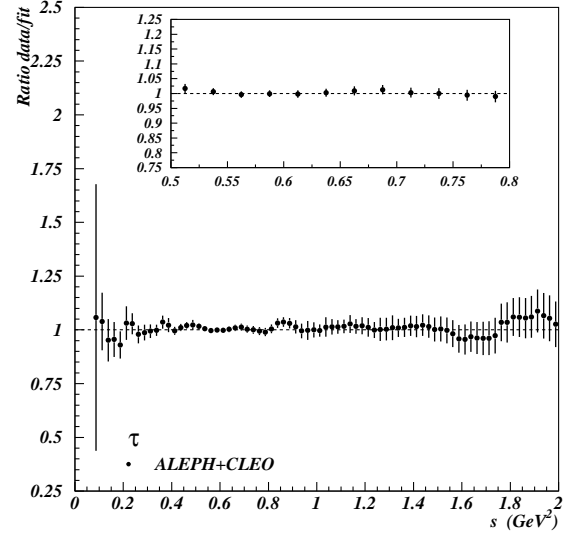


Figure 3. The ratio of the  $\tau$  pion form factor squared to  $|F_\pi^-(s)|^2$  from the combined fit in Table 3.

should be well predicted by QCD as it is an inclusive observable. Compared to the similar quantity defined in  $e^+e^-$  annihilation, it is even twice inclusive: not only are all produced hadronic states at a given mass summed over, but an integration is performed over all the possible masses from  $m_\pi$  to  $m_\tau$ .

This favourable situation could be spoiled by the fact that the  $Q^2$  scale is rather small, so that questions about the validity of a perturbative approach can be raised. At least two levels are to be considered: the convergence of the perturbative expansion and the control of the nonperturbative contributions. Happy circumstances make these latter components indeed very small [23–25].

The perturbative expansion (FOPT) is known to third order [27]. A resummation of all known higher order logarithmic integrals improves the convergence of the perturbative series (contour-improved method FOPT<sub>CI</sub>) [28]. As some ambiguity persists, the results are given as an average

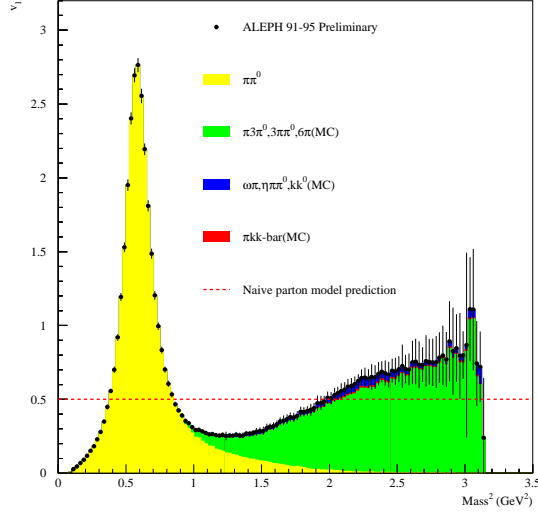


Figure 4. Preliminary ALEPH inclusive vector spectral function with its different contributions. The dashed line is the expectation from the naive parton model.

of the two methods with the difference taken as a systematic uncertainty. The small nonperturbative contributions are parametrized using the Operator Product Expansion (OPE) [26].

## 5.2. Results of the Fits

The QCD analysis of the  $\tau$  hadronic width has not yet been completed with the final ALEPH spectral functions. Results given below correspond to the published analyses with a smaller data set.

The ratio  $R_\tau$  is obtained from measurements of the leptonic branching ratios:

$$R_\tau = 3.647 \pm 0.014 \quad (8)$$

using a value  $B(\tau^- \rightarrow e^- \bar{\nu}_e \nu_\tau) = (17.794 \pm 0.045)\%$  which includes the improvement in accuracy provided by the universality assumption of leptonic currents together with the measurements of  $B(\tau^- \rightarrow e^- \bar{\nu}_e \nu_\tau)$ ,  $B(\tau^- \rightarrow \mu^- \bar{\nu}_\mu \nu_\tau)$  and the  $\tau$  lifetime. The nonstrange part of  $R_\tau$  is obtained by subtracting out the measured strange contribution (see last section). The results of the

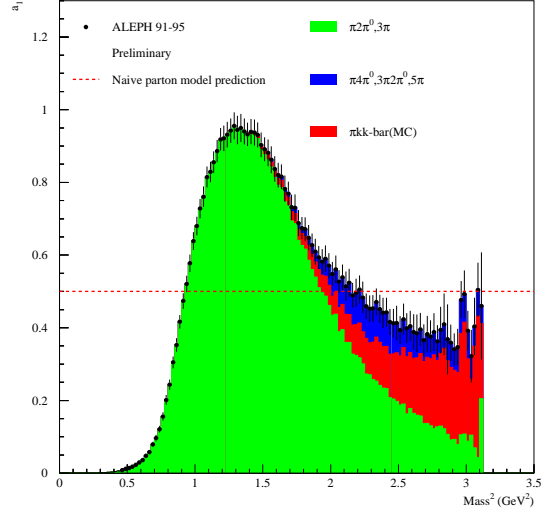


Figure 5. Preliminary ALEPH inclusive axial-vector spectral function with its different contributions. The dashed line is the expectation from the naive parton model.

fits are given in Table 4 for the ALEPH analysis.

One notices a remarkable agreement within statistical errors between the  $\alpha_s(m_\tau^2)$  values using vector and axial-vector data. The total nonperturbative power contribution to  $R_{\tau,V+A}$  is compatible with zero within an uncertainty of 0.4%, that is much smaller than the error arising from the perturbative term. This cancellation of the nonperturbative terms increases the confidence on the  $\alpha_s(m_\tau^2)$  determination from the inclusive  $(V+A)$  observables.

The final result from ALEPH is :

$$\alpha_s(m_\tau^2) = 0.334 \pm 0.007_{\text{exp}} \pm 0.021_{\text{th}} \quad (9)$$

where the first error accounts for the experimental uncertainty and the second gives the uncertainty of the theoretical prediction of  $R_\tau$  and the spectral moments as well as the ambiguity of the theoretical approaches employed.

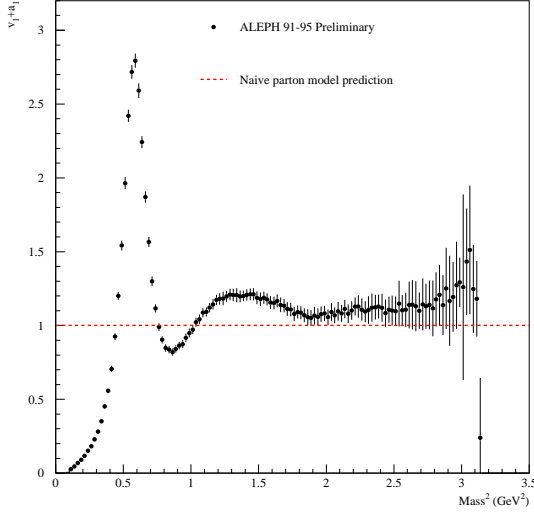


Figure 6. The preliminary inclusive  $V + A$  nonstrange spectral function from ALEPH. The dashed line is the expectation from the naive parton model.

### 5.3. Test of the Running of $\alpha_s(s)$ at Low Energies

Using the spectral functions, one can simulate the physics of a hypothetical  $\tau$  lepton with a mass  $\sqrt{s_0}$  smaller than  $m_\tau$  and hence further investigate QCD phenomena at low energies. Assuming quark-hadron duality, the evolution of  $R_\tau(s_0)$  provides a direct test of the running of  $\alpha_s(s_0)$ , governed by the RGE  $\beta$ -function. On the other hand, it is a test of the validity of the OPE approach in  $\tau$  decays.

In practice, the experimental value for  $\alpha_s(s_0)$  has been determined at every  $s_0$  from the comparison of data and theory. Good agreement is observed with the four-loop RGE evolution using three quark flavours (Fig. 7). The experimental fact that the nonperturbative contributions cancel over the whole range  $1.2 \text{ GeV}^2 \leq s_0 \leq m_\tau^2$  leads to confidence that the  $\alpha_s$  determination from the inclusive  $(V + A)$  data is robust.

ALEPH	$\alpha_s(m_\tau^2)$	$\delta_{\text{NP}}$
V	$0.330 \pm 0.014 \pm 0.018$	$0.020 \pm 0.004$
A	$0.339 \pm 0.013 \pm 0.018$	$-0.027 \pm 0.004$
V+A	$0.334 \pm 0.007 \pm 0.021$	$-0.003 \pm 0.004$

Table 4

Fit results of  $\alpha_s(m_\tau^2)$  and the OPE nonperturbative contributions from vector, axial-vector and  $(V + A)$  combined fits using the corresponding ratios  $R_\tau$  and the spectral moments as input parameters. The second error is given for theoretical uncertainty.

### 5.4. Evolving $\alpha_s$ from $m_\tau$ to $M_Z$

The evolution of the  $\alpha_s(m_\tau^2)$  measurement from the inclusive  $(V + A)$  observables based on the Runge-Kutta integration of the differential equation of the renormalization group to N<sup>3</sup>LO [29,31] yields for the ALEPH analysis

$$\alpha_s(M_Z^2) = 0.1202 \pm 0.0008_{\text{exp}} \pm 0.0024_{\text{th}} \pm 0.0010_{\text{evol}} \quad (10)$$

where the last error stands for possible ambiguities in the evolution due to uncertainties in the matching scales of the quark thresholds [31]. The result (10) can be compared to the precise determination from the measurement of the  $Z$  width, as obtained in the global electroweak fit. The variable  $R_Z$  has similar advantages to  $R_\tau$ , but it differs concerning the convergence of the perturbative expansion because of the much larger scale. It turns out that this determination is dominated by experimental errors with very small theoretical uncertainties, *i.e.* the reverse of the situation encountered in  $\tau$  decays. The most recent value [32] yields  $\alpha_s(M_Z^2) = 0.1183 \pm 0.0027$ , in excellent agreement with (10). Fig. 7 illustrates well the agreement between the evolution of  $\alpha_s(m_\tau^2)$  predicted by QCD and  $\alpha_s(M_Z^2)$ .

## 6. Strange Spectral Function and Strange Quark Mass

The spectral function for strange final states has been determined by ALEPH [5]: it is dominated by the vector  $K^*(890)$  and higher mass (mostly axial-vector) resonances. The total rate for strange final states, using the complete



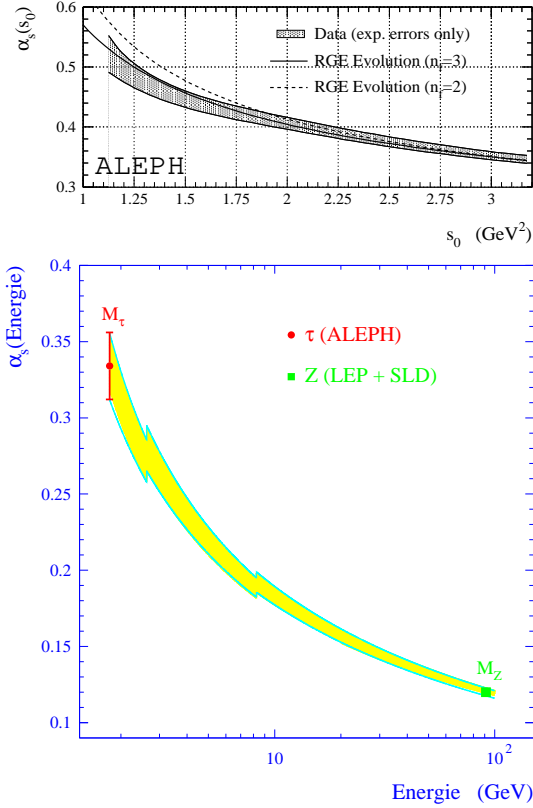


Figure 7. The running of  $\alpha_s(s_0)$  obtained from the fit of the theoretical prediction to  $R_{\tau,V+A}(s_0)$  below the  $\tau$  mass in the top plot: the shaded band shows the data including experimental errors, while the curves give the four-loop RGE evolution for two and three flavours. The plot below shows the evolution of the strong coupling (measured at  $m_\tau^2$ ) to  $M_Z^2$  predicted by QCD compared to the direct measurement. Flavour matching is accomplished at 3 loops at  $2 m_c$  and  $2 m_b$  thresholds.

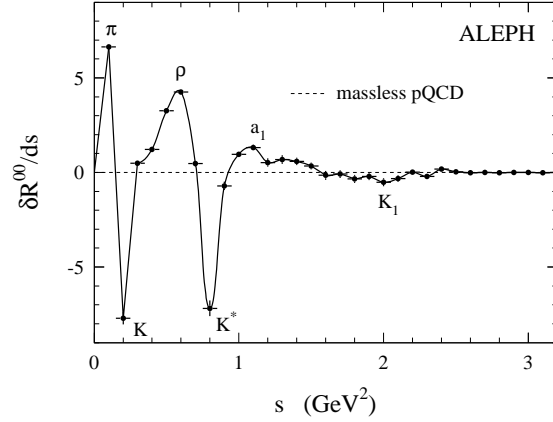


Figure 8. Differential rate for  $\Delta_\tau^{00}$ , difference between properly normalized nonstrange and strange spectral functions (see text for details). The contribution from massless perturbative QCD vanishes. To guide the eye, the solid line interpolates between bins of constant  $0.1 \text{ GeV}^2$  width.

ALEPH analyses supplemented by results from other experiments [33] is determined to be  $B(\tau \rightarrow \nu_\tau \text{hadrons}_{S=-1}) = (29.3 \pm 1.0) 10^{-3}$ , leading to

$$R_{\tau,S} = 0.163 \pm 0.006. \quad (11)$$

Spectral moments are again useful tools to unravel the different components of the inclusive rate. Since we are mostly interested in the specific contributions from the  $\bar{u}s$  strange final state, it is useful to form the difference

$$\Delta_\tau^{kl} \equiv \frac{1}{|V_{ud}|^2} R_{\tau,S=0}^{kl} - \frac{1}{|V_{us}|^2} R_{\tau,S=-1}^{kl} \quad (12)$$

where the flavour-independent perturbative part and gluon condensate cancel. Fig. 8 shows the interesting behaviour of  $\Delta_\tau^{00}$  expressed differentially as a function of  $s$ . The leading QCD contribution to  $\Delta_\tau^{kl}$  is a term proportional to the square of the strange quark mass at the  $\tau$  energy scale. We quote here the recent result from the analysis of Ref. [34], yielding

$$m_s(m_\tau^2) = (120 \pm 11_{\text{exp}} \pm 8_{V_{us}} \pm 19_{th}) \text{ MeV} \quad (13)$$

where the dominant uncertainty is from theory, mostly because of the poor convergence behaviour.

## 7. Conclusions

The decays  $\tau \rightarrow \nu_\tau + \text{hadrons}$  constitute a clean and powerful way to study hadronic physics up to  $\sqrt{s} \sim 1.8$  GeV. Beautiful resonance analyses have already been done, providing new insight into hadron dynamics. Probably the major surprise has been the fact that inclusive hadron production is well described by perturbative QCD with very small nonperturbative components at the  $\tau$  mass. In spite of the fact that this low-energy region is dominated by resonance physics, methods based on global quark-hadron duality work indeed very well.

The ALEPH preliminary results using the full LEP1 sample have been presented. Satisfactory agreement with CLEO is observed in the  $\pi\pi^0$  decay mode. The  $\tau$  spectral functions have now reached a precision level where detailed investigations are possible, particularly in the most interesting  $\pi\pi^0$  channel. The breaking of SU(2) symmetry can be directly determined through the comparison between  $e^+e^-$  and  $\tau$  spectral functions. In particular, the possibility of a  $\rho$  mass splitting between neutral and charged states is carefully investigated. The data tend to favour non-degenerate states with  $m_{\rho^-} - m_{\rho^0} = (2.3 \pm 0.8)$  MeV. Correcting the  $\tau$  spectral function for this additional isospin breaking leaves an overall normalization difference of 3.3% with  $e^+e^-$  data, thus enhancing the existing discrepancy for  $a_\mu^{\text{had,LO}}$ . The situation must be revisited with new high precision  $e^+e^-$  data [20,35].

The measurement of the vector and axial-vector spectral functions has provided the way for quantitative QCD analyses. These spectral functions are very well described in a global way by  $O(\alpha_s^3)$  perturbative QCD with small nonperturbative components. Precise determinations of  $\alpha_s$  agree for both spectral functions and they also agree with all the other determinations from the Z width, the rate of Z to jets and deep inelastic lepton scattering. Indeed from  $\tau$  decays,  $\alpha_s(M_Z^2)_\tau = 0.1202 \pm 0.0027$ , in excellent agree-

ment with the average from all other determinations [36],  $\alpha_s(M_Z^2)_{\text{non-}\tau} = 0.1187 \pm 0.0020$ .

The strange spectral function yields a value for the strange quark mass which can be evolved to the usual comparison scale,  $m_s(2 \text{ GeV}) = (116_{-25}^{+20})$  MeV.

The  $\tau$  spectral functions have been shown to be a privileged field for the study of QCD.

## Acknowledgments

I would like to thank Shaomin Chen, Andreas Höcker, Changzheng Yuan and Zhiqing Zhang for their many contributions to this work. Congratulations to Marco Incagli and Graziano Venanzoni for organizing a very stimulating workshop.

## REFERENCES

1. Review of Particle Properties, *Phys.Rev.* **D66** (2002) 010001.
2. M. Davier and C. Yuan, *Nucl.Phys. B* (Proc.Suppl.) **123** (2003) 47.
3. R. Barate *et al.* (ALEPH Collaboration), *Z.Phys.* **C76** (1997) 15.
4. ALEPH Collaboration, *Eur.Phys.J.* **C4** (1998) 409.
5. ALEPH Collaboration, *Eur.Phys.J.* **C11** (1999) 599.
6. T. Bergfeld *et al.*, CLEO Coll., *Phys.Rev.Lett.* **79** (1997) 2406; A. Weinstein, Proceedings of the 6<sup>th</sup> International Workshop on  $\tau$  Lepton Physics, Victoria, R. J. Sobie and J. M. Roney eds., North Holland (2001)
7. S. Anderson *et al.* (CLEO Collaboration), *Phys.Rev.* **D61**(2000) 112002.
8. W. Marciano and A. Sirlin, *Phys.Rev.Lett.* **61** (1988) 1815.
9. E. Braaten and C.S. Li, *Phys.Rev.* **42** (1990) 3888.
10. R. Decker and M. Finkenmeier, *Nucl.Phys.* **438** (1995) 17.
11. V. Cirigliano, G. Ecker and H. Neufeld, *Phys. Lett.* **B513** (2001) 361; V. Cirigliano, G. Ecker and H. Neufeld, *JHEP* **0208** (2002) 002.
12. R. Alemany, M. Davier and A. Höcker, *Eur.Phys.J.* **C2** (1998) 123.

13. H. Czyż and J.H. Kühn, *Eur.Phys.J.* **C18** (2001) 497.
14. M. Davier, S.I. Eidelman, A. Höcker and Z. Zhang, *Eur.Phys.J.* **C11** (1999) 599.
15. G.J. Gounaris and J.J. Sakurai, *Phys. Rev. Lett.* **21** (1968) 244.
16. J. Bijnens and P. Gosdzinsky, *Phys. Lett.* **B388** (1996) 203.
17. R.R. Akhmetshin *et al.* (CMD-2 Collaboration), hep-ex/0308008 (August 2003).
18. M. Davier, S.I. Eidelman, A. Höcker and Z. Zhang, hep-ph/0308213 (August 2003), to appear in *Eur.Phys.J.*
19. F. Guerrero and A. Pich, *Phys. Lett.* **B412** (1997) 382; D. Gómez Gumm, A. Pich and J. Portolés, *Phys.Rev.* **62** (2000) 054014.
20. B. Valeriani, *Preliminary results from KLOE on the radiative return*, these proceedings.
21. M. Davier, *Hadronic vacuum polarization and the muon magnetic moment*, these proceedings.
22. OPAL Collaboration, *Eur.Phys.J.* **C7** (1999) 571.
23. E. Braaten, *Phys.Rev.Lett.* **60** (1988) 1606.
24. S. Narison and A. Pich, *Phys.Lett.* **B211**(1988) 183.
25. E. Braaten, S. Narison and A. Pich, *Nucl.Phys.* **B373** (1992) 581.
26. M.A. Shifman, A.L. Vainshtein and V.I. Zakharov, *Nucl.Phys.* **B147** (1979) 385; *ibid* **B147** (1979) 448; *ibid* **B147** (1979) 519.
27. L.R. Surguladze and M.A. Samuel, *Phys. Rev. Lett.* **66** (1991) 560; S.G. Gorishny, A.L. Kataev and S.A. Larin, *Phys. Lett.* **B259** (1991) 144.
28. F. Le Diberder and A. Pich, *Phys. Lett.* **B286** (1992) 147.
29. S.A. Larin, T. van Ritbergen and J.A.M. Vermaseren, *Phys. Lett.* **B400** (1997) 379. K.G. Chetyrkin, B.A. Kniehl and M. Steinhauser, *Nucl.Phys.* **B510** (1998) 61. W. Bernreuther, W. Wetzel, *Nucl.Phys.* **B197** (1982) 228. W. Wetzel, *Nucl.Phys.* **B196** (1982) 259. W. Bernreuther, PITHA-94-31 (1994).
30. K.G. Chetyrkin, B.A. Kniehl and M. Steinhauser, *Phys. Rev. Lett.* **79** (1997) 2184.
31. G. Rodrigo, A. Pich, A. Santamaria, *Phys.Lett.* **B424** (1998) 367.
32. LEPEWWG/2002-02, hep-ex/0212036 (December 2002).
33. M. Davier, S. Chen, A. Höcker, J. Prades and A. Pich, *Nucl.Phys.* (Proc. Suppl.) **B98** (2001) 319.
34. S. Chen, M. Davier, E. Gámiz, A. Höcker, J. Prades and A. Pich, *Eur.Phys.J.* **C22** (2002) 31.
35. M. Davier, *R measurement through ISR with BaBar*, these proceedings.
36. M. Davier, '98 Rencontres de Moriond on Electroweak Interactions, Ed. J. Trân Thanh Vân, Frontières, Paris (1998).